# Human Sco1 functional studies and pathological implications of the P174L mutant

Lucia Banci*†, Ivano Bertini*‡, Simone Ciofi-Baffoni*, Iliana Leontari*, Manuele Martinelli*, Peep Palumaa§, Rannar Sillard§¶, and Shenlin Wang*

*Magnetic Resonance Center (CERM) and Department of Chemistry, University of Florence, Via Luigi Sacconi 6, 50019 Sesto Fiorentino, Florence, Italy; †FiorGen Foundation, Via Luigi Sacconi 6, 50019 Sesto Fiorentino, Florence, Italy; ¶Department of Medical Biochemistry and Biophysics, Karolinska Institutet, SE-171 77 Stockholm, Sweden; and §Department of Gene Technology, Tallinn University of Technology, Akadeemia tee 15, 12618 Tallinn, Estonia

Edited by Joan Selverstone Valentine, University of California, Los Angeles, CA, and approved October 30, 2006 (received for review July 21, 2006)

**The pathogenic mutant (P174L) of human Sco1 produces respiratory chain deficiency associated with cytochrome *c* oxidase (CcO) assembly defects. The solution structure of the mutant in its Cu(I) form shows that Leu-174 prevents the formation of a well packed hydrophobic region around the metal-binding site and causes a reduction of the affinity of copper(I) for the protein. $K_D$ values for Cu(I)WT-HSco1 and Cu(I)P174L-HSco1 are $\approx 10^{-17}$ and $\approx 10^{-13}$, respectively. The reduction potentials of the two apo proteins are similar, but slower reduction/oxidation rates are found for the mutant with respect to the WT. The mitochondrial metallochaperone in the partially oxidized $Cu_1(I)Cox17_{2S\text{-}S}$ form, at variance with the fully reduced $Cu_4(I)Cox17$, interacts transiently with both WT-HSco1 and the mutant, forming the Cox17/Cu(I)/HSco1 complex, but copper is efficiently transferred only in the case of WT protein. $Cu_1(I)Cox17_{2S\text{-}S}$ indeed has an affinity for copper(I) ($K_D \approx 10^{-15}$) higher than that of the P174L-HSco1 mutant but lower than that of WT-HSco1. We propose that HSco1 mutation, altering the structure around the metal-binding site, affects both copper(I) binding and redox properties of the protein, thus impairing the efficiency of copper transfer to CcO. The pathogenic mutation therefore could (*i*) lessen the Sco1 affinity for copper(I) and hence copper supply for CcO or (*ii*) decrease the efficiency of reduction of CcO thiols involved in copper binding, or both effects could be produced by the mutation.**

cytochrome *c* oxidase | mass spectrometry | NMR | copper chaperone | respiratory chain deficiency

Cytochrome *c* oxidase (CcO) is the terminal enzyme of the respiratory chain, embedded in the inner mitochondrial membrane of all eukaryotes and in the plasma membrane of many prokaryotes. In eukaryotes, a large number of nuclear genes are required for the proper assembly and function of the CcO complex, among which at least six proteins (Cox17, Cox23, Cox19, Sco1, Sco2, and Cox11) are involved in the delivery and insertion of copper into the binuclear $Cu_A$ and $Cu_B$-heme $a_3$ sites of CcO (1–3). Sco1 and Sco2, which are anchored to the inner mitochondrial membrane through a single transmembrane helix, are specifically implicated in the assembly of the $Cu_A$ site of CcO (4–7). Sco1 and Sco2 are both metal-binding proteins capable to bind either copper(I) or copper(II) in the same metal-binding site (8, 9); mutations of the ligands that abrogate their copper-binding ability drastically compromise CcO activity (9, 10). The mitochondrial copper chaperone Cox17 is capable of donating copper(I) to Sco1 (11), implying that it might transfer copper to Sco1, which, in turn, inserts it into the $Cu_A$ site. According to this mechanism, Sco1 was shown to interact with the $Cu_A$-containing COXII subunit of CcO (6).

Important insights on the function of this class of proteins also recently were obtained from a genome-wide search for all available prokaryotic genomes (12). This search showed the presence of several Sco paralogs adjacent to copper and/or redox proteins, thus suggesting that Sco proteins can have multifunctional properties involved in different physiological processes.

The structure of Sco proteins is characterized by a thioredoxin fold (13–15), and, from the first structural characterization (13), it was suggested that the protein also may fulfill a redox function. Recently, we have solved the solution structures of the demetallated, the copper(I), and the nickel(II) derivatives of human Sco1 (HSco1 hereafter) as well as the crystal structure of a nickel(II) derivative (16). The structural analysis showed that Cu(I) is coordinated by ligands located in two distant protein regions: Cys-169 and Cys-173 of the CXXXC conserved motif in loop 3 and His-260 in loop 8. In the structure of the apo protein, the latter loop is highly disordered and mobile in solution (16), suggesting that the metal binding is able to "freeze" this loop in a more rigid conformation, thus representing an important step in the metal-binding process of HSco1. In the crystal structure of oxidized Ni(II)HSco1, the two metal-binding cysteines are oxidized and form a disulfide bond, still with the metal ion interacting with the S-S moiety. This metal environment showed that the protein can have a peculiar mode of interaction with a metal ion, suggesting that cysteine oxidation of HSco1 also might play a role in the metal release to $Cu_A$ site of CcO (16). These structural data further support our initial suggestion that Sco1 can act both as a copper chaperone and a thioredoxin (13).

Human *SCO1* and *SCO2* genes can experience pathogenic mutations that produce respiratory chain deficiency associated with CcO assembly defects (17). The missense mutation in human Sco1 gene of a proline into a leucine, P174L, is associated with a fatal neonatal hepatopathy when the second allele also is nonfunctional (18). This finding implies that the pathology is caused by a loss of normal Sco1 function rather than gain of some aberrant action of the mutant protein. This proline, adjacent to the conserved CXXXC domain of HSco1, is completely conserved in eukaryotes. Introduction of the P174L mutant chimeric HSco1 protein in Sco1-null yeast mutants impaired CcO assembly and induced loss of CcO activity (19). WT protein and P174L mutant chimera are present in comparable concentrations in mitochondrial extracts, thus indicating that the pathogenicity of the mutant does not result from its instability but rather from an impaired function (19). During the preparation of our work, a paper on the same P174L-HSco1 mutant came out indicating that the mutation compromises Cox17-dependent metalation

Author contributions: L.B., I.B., S.C.-B., and P.P. designed research; S.C.-B., I.L., M.M., P.P., and S.W. performed research; R.S. contributed new reagents/analytic tools; S.C.-B., M.M., P.P., and S.W. analyzed data; and L.B., I.B., S.C.-B., and P.P. wrote the paper.

The authors declare no conflict of interest.

This article is a PNAS direct submission.

Abbreviations: CcO, cytochrome *c* oxidase; HSQC, heteronuclear single quantum correlation; ESI, electrospray ionization; GSH, reduced glutathione; GSSG, oxidized glutathione.

Data deposition: The atomic coordinates and structural restraints for human Cu(I)P174LSco1 structure have been deposited in the Protein Data Bank, www.pdb.org (PDB ID code 2HRN).

‡To whom correspondence should be addressed. E-mail: bertini@cerm.unifi.it.

This article contains supporting information online at www.pnas.org/cgi/content/full/0606189103/DC1.

without impairing copper binding (20). In the present research, we have explored at the molecular level the effect of the mutation on the Sco1 function by solving the solution structure of the P174L-HSco1 mutant, characterizing the metal-binding and redox properties of the P174L-HSco1 mutant with respect to WT HSco1 (WT-HSco1 hereafter), and investigating the role of Cox17 in the copper transfer to both WT and mutant HSco1 proteins. Our work demonstrates that the P174L mutation alters hydrophobic interactions around the metal-binding site, thus affecting both the copper-binding and the redox properties of HSco1 and, therefore, determining a reduction of the copper transfer efficiency from Cox17 to HSco1. We also learned that the partially oxidized $Cu_1(I)Cox17_{2S\text{-}S}$ and not the fully reduced $Cu_4(I)Cox17$ are the preferential species delivering copper to HSco1.

## Results

**Structural Properties of the Pathogenic Mutant P174L-HSco1.** ApoP174L-HSco1 at millimolar concentration is a well folded protein as it appears from the $^1H$-$^{15}N$ heteronuclear single quantum correlation (HSQC) spectrum [see supporting information (SI) Fig. 5], which also is similar to that of apoWT-HSco1. Accordingly, the mutant maintains the same fold of WT-HSco1, featuring indeed the same content of $\beta$-strands (21%) and $\alpha$-helices (26%) as derived from circular dichroism spectra. Fluorimetric thermal unfolding assay (SI Fig. 5) shows that the thermal stability of apoP174L-HSco1 also is the same as that of apoWT-HSco1, both having a melting temperature of ≈54°C. These data show that the pathogenic nature of the mutation does not originate from fold and/or stability differences of apoP174L-HSco1 with respect to the WT protein. This conclusion also is consistent with *in vivo* results, which showed that comparable concentrations of either WT or P174L mutant protein are present in mitochondrial extracts (19).

ApoP174L-HSco1, as apoWT-HSco1, is able to bind Cu(I) ions, when the latter is provided as Cu(I) acetonitrile complex. The metalation of both proteins, followed through $^1H$-$^{15}N$ HSQC spectra in the presence of 1 mM DTT (SI Fig. 6), however, shows meaningful differences. Indeed, although 1 eq of Cu(I) fully metallates WT-HSco1, complete metalation of P174L-HSco1 is not achieved even when 3 eq of Cu(I) are added, as ≈20% of P174L-HSco1 is still in the apo form (SI Fig. 6). In the latter experiment, Cu(I) thus competes between the mutant and the DTT chelator, allowing us to determine the dissociation constant ($K_D$) of the Cu(I)P174L-HSco1 complex. Following the relative ratio of apo and copper(I) forms, as obtained from the $^1H$-$^{15}N$ HSQC spectra of the mixture during the titration steps [the interaction between the protein and Cu(I)DTT complex is slow on the chemical-shift time scale], $K_D$ of the Cu(I)P174L-HSco1 complex is estimated to be $3.2 \pm 0.6 \times 10^{-13}$ M. This value is much higher than the $K_D \approx 10^{-17}$ of the WT protein (see *Transfer of Copper from Cox17 to HSco1*). When copper(I) is added in the absence of DTT, 1.5 eq are enough to fully metallate the mutant.

Copper binding to WT-HSco1 induces major conformational changes to the protein, which passes from an open state in the apo form to a closed, compact one upon copper binding (16). This change clearly is evident from the solution structures of these two states of WT-HSco1 and also can readily be assessed from the charge state analysis of electrospray ionization (ESI)-MS spectra. Conformational analysis by ESI-MS is based on observation that, during the ESI, tightly compact proteins acquire only a narrow range of low-charge values, whereas open conformations produce a more heterogeneous and highly charged population (21). Charge-state distribution of Cu(I)P174L-HSco1 ($Int_{+9}/Int_{+10} = 1.6$; Fig. 1) is similar to that of apoP174L-HSco1 ($Int_{+9}/Int_{+10} = 1.7$) and apoWT-HSco1 ($Int_{+9}/Int_{+10} = 1.4$), indicating that all these systems have a more

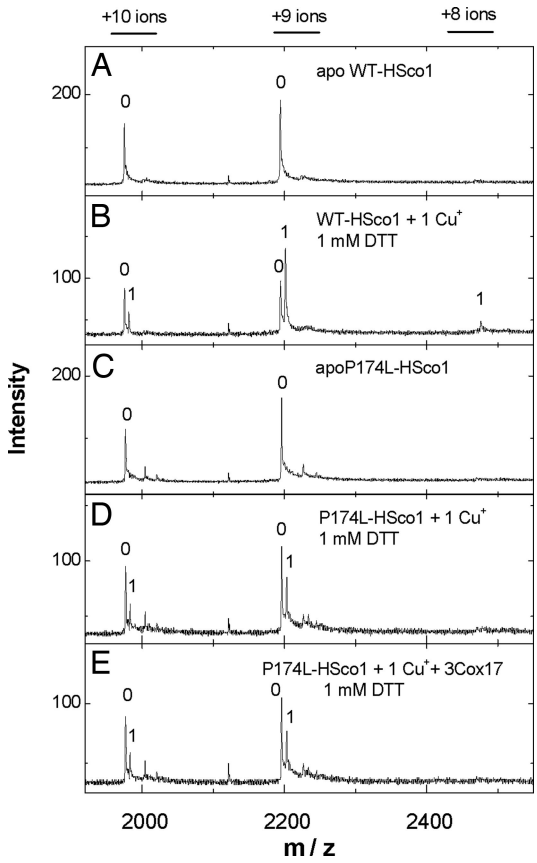


**Fig. 1.** Binding of copper ions to human Sco1 and mutant P174LSco1. ESI-TOF mass spectra of WT-HSco1 (0.8 $\mu$M) and P174L-HSco1 (1.2 $\mu$M) reconstituted with Cu(I)DTT complex in 50 mM ammonium acetate, pH 7.5. (*A*) apoWT-HSco1. (*B*) WT-HSco1 + 1 eq of Cu(I) in the presence of 1.0 mM DTT. (*C*) apoP174L-HSco1. (*D*) P174L-HSco1 + 1 eq of Cu(I) in the presence of 1.0 mM DTT. (*E*) P174L-HSco1 + 1 eq of Cu(I) + 3 eq of $Cox17_{2S\text{-}S}$ in the presence of 1.0 mM DTT. Charge state +8, +9, and +10 ions are presented and numbers on the peaks denote the metal stoichiometry of the complex.

open conformation than Cu(I)WT-HSco1, in which the lower +9 state was more populated ($Int_{+9}/Int_{+10} = 3.8$; Fig. 1). These data therefore show that Cu(I) binding to apoP174L-HSco1 is unable to induce the compact conformation as it occurs in the WT protein.

In the $^1H$-$^{15}N$ HSQC spectrum of the fully metallated P174L-HSco1 ($Cu_1(I)$P174L-HSco1), 34 residues show a splitting in two or, in a few cases, three NH cross-peaks, indicating the occurrence of structural heterogeneity, which is absent in $Cu_1(I)$WT-HSco1. The two major species are present in a ratio of 60:40. The relative intensity of the resonances of the two species is temperature-dependent, indicating that there is an equilibrium between the two. The solution structure of $Cu_1(I)$P174L-HSco1 (determined from the more abundant species) shows the same thioredoxin-like fold of the WT protein (Fig. 2) with an average backbone rmsd of 1.30 Å. The only significant structural difference is in loop 8, which contains the His copper ligand. In the mutant, this loop does not have the short $\beta$-hairpin (Fig. 2), similarly to what occurs in the apoWT-HSco1 solution structure but at variance with the $Cu_1(I)$WT-HSco1 structure (16). Because no apo form of the mutant is present in the NMR sample (see *Methods*), the latter less defined secondary structure could be the consequence of the structural heterogeneity in this region, which in turn could induce a weaker copper-affinity in the mutant. Several residues with double conformations are located in helix $\alpha$2, which is in contact with the metal-binding CXXXC

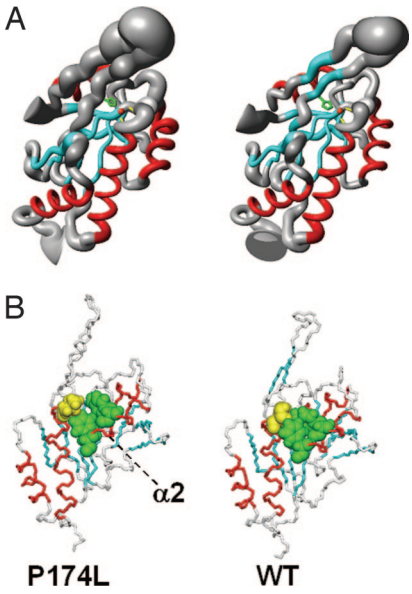


**Fig. 2.** Solution structure of $Cu_1$(I)P174L-HSco1 mutant. (*A*) Backbone atoms are represented as a tube with variable radius, proportional to the backbone rmsd value of each residue for $Cu_1$(I)P174L-HSco1 and $Cu_1$(I)WT-HSco1. The side chains of Cys-169, Cys-173, His-260, and the copper(I) ions are shown in yellow, green, and orange, respectively. The secondary structure elements also are indicated: $\beta$-strands are in cyan and $\alpha$-helices in red. (*B*) Side-chain packing involving Pro-174 or Leu-174 (in yellow) and Tyr-216 and Phe-220 (in green) is shown on the WT and P174L mean minimized solution structures. The mutant protein was copper-saturated resulting in a 1:1 copper:protein complex.

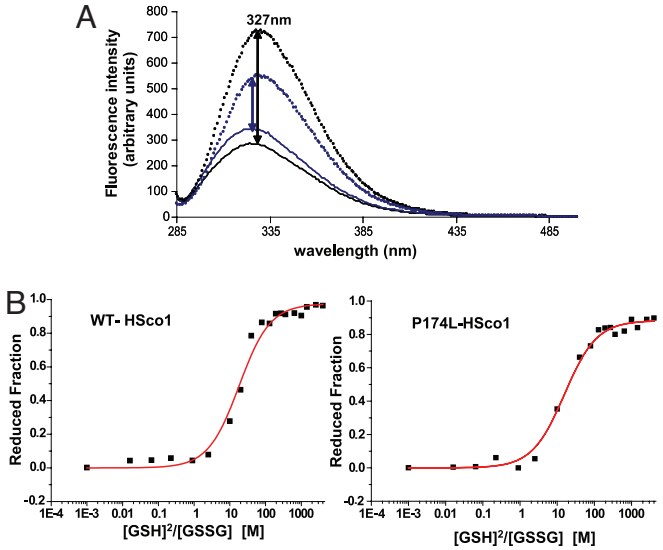


**Fig. 3.** Redox properties of WT-HSco1 and P174L-HSco1. (*A*) Fluorescence emission spectra of 5 $\mu$M WT-HSco1 (black) and P174L-HSco1 (blue) recorded under native conditions of the oxidized (50 mM phosphate buffer, pH 7.0, 0.01 mM GSSG; dotted lines) and the reduced (50 mM phosphate buffer, pH 7.0, 200 mM GSH; solid lines) protein after excitation at 280 nm. (*B*) Redox equilibrium of WT-HSco1 and P174L-HSco1 with different $[GSH]^2$/GSSG ratios as followed by measuring fluorescence emission at 327 nm. After nonlinear regression, values of $K_{eq}$ = 17.70 ± 2.23 mM and of 15.66 ± 1.86 mM (correlation coefficient: 0.986 and 0.996) were obtained for the WT-HSco1 and P174L-HSco1/glutathione systems, corresponding to a redox potentials of −0.277 ± 0.030 V and −0.275 ± 0.028 V, respectively, by using the glutathione standard potential of −0.240 V at pH 7.0 and 298 K.

region through hydrophobic interactions involving Leu-174 or Pro-174 and Leu-177 (helix $\alpha$1), and Tyr-216 and Phe-220 (helix $\alpha$2). Although Pro-174 has extensive hydrophobic contacts with both Tyr-216 and Phe-220 in $Cu_1$(I)WT-HSco1, thus forming a compact hydrophobic patch, in the mutant, the bulkier Leu side chain prevents the optimal packing with the two aromatic side chains (Fig. 2), which indeed display double conformation. Leu-174 essentially interacts only with Phe-220 (Fig. 2) and is more solvent-exposed (25%) than Pro-174 is (12%). The lack of a well organized hydrophobic core on this side of the metal-binding region also causes the presence of a double conformation for His-260, located in loop 8. Two patterns for the aromatic ring of this His are observed in the $^2J_{NH}$ coupling-based $^1H$-$^{15}N$ HSQC spectra (SI Fig. 7). One pattern, belonging to the minor species, fully matches the shifts of His-260 in $Cu_1$(I)WT-HSco1, whereas the other has different shifts but still is indicative of copper(I) coordination through N$\varepsilon$2 as in the WT protein. In the major species, His-260 lacks NOEs contacts with the CXXXC metal-binding region that are present in the WT form. A decreased number of NOEs with respect to WT protein also is observed in the metal-binding loop 3 and in the surrounding loops 5, 7, and 8, likely reflecting the effect of the observed conformational disorder. From this structural investigation, we thus can conclude that the mutation (*i*) perturbs the hydrophobic interactions and (*ii*) induces conformational heterogeneity around the copper-binding site, with both effects overall reducing the affinity of the protein for copper(I).

**Redox Properties of the Pathogenic Mutant P174L-HSco1.** Based on its thioredoxin fold, it has been suggested that the two Cys residues of the CXXXC conserved motif in Sco protein family can be involved in redox reactions (13–15), perhaps in the reduction of the oxidized cysteines in $Cu_A$ site of CcO (16). Oxidized and reduced forms of apoHSco1 are characterized by different fluorescence spectra (Fig. 3). Trp-159 and, to a lesser extent, Tyr-163 are the residues principally contributing to the difference of florescence intensity upon change of the oxidation state of the protein (see *SI Text* for details), as assessed by comparing the fluorescence spectra of W159F, W159F/Y163F, and Y216F mutants with that of WT-HSco1 (SI Fig. 8). Tyr-163 is close to the CXXXC motif, whereas Trp-159 is far but still belonging to the same $\beta$-strand of Tyr-163. From the difference in fluorescence of the two redox states of the protein, the reduction potential of the two cysteines for WT- and P174L-HSco1 in their apo forms can be determined. The measured reduction potentials at pH 7.2 are −0.277 ± 0.030 V and −0.275 ± 0.028 V for WT-HSco1 and P174L-HSco1, respectively (Fig. 3), falling in the standard state redox potentials range of the thioredoxin family of thiol-disulfide oxidoreductases (−124 to −270 mV) (22), consistently with a possible function of HSco1 as a thioredoxin. The similar reduction potentials of WT-HSco1 and P174L-HSco1 also indicate that the pathogenic mutation does not significantly affect the thermodynamic equilibrium between reduced and oxidized HSco1. However, the kinetic rates of disulfide bond formation and reduction are significantly different in WT-HSco1 and P174L-HSco1 forms. Air oxidation of cysteines in apoWT-HSco1 has an half-life time of ≈4 h. Oxidation of apoP174L-HSco1 is a much slower process, because ≈70% of the reduced form still is present after 4 h of air exposure (SI Fig. 9). Reduction of the disulfide bond in oxidized apoHSco1, by 1 mM DTT, also has different rates in the two proteins, being much faster in WT-HSco1 than in the mutant. In the former, the reduction of the disulfide bond is completed already after 1 min (SI Fig. 10); however, after the same period, only 20% of oxidized apoP174L-HSco1 is reduced, and, after 5 min, a reduction level of only 55% is reached (SI Fig. 10). In summary, P174L-HSco1 mutant has a similar redox potential as compared with WT protein but significantly slower reduction and oxidation rates.

**Transfer of Copper from Cox17 to HSco1.** After the characterization of the structural and redox properties of the P174L-HSco1 mutant, we also addressed and analyzed the mechanism of copper acquisition from the copper chaperone Cox17, which also could be affected by the mutation. For this analyses, we have used porcine Cox17, which differs from human Cox17 only in the first four amino acid residues. Cox17 could exist in three different oxidation states, which have different metal-binding properties (23). In oxidative environment, a completely oxidized form with three disulfide bonds ($Cox17_{3S\text{-}S}$ hereafter) is present that is unable to bind copper. In the presence of 1 mM DTT, Cox17 is partially oxidized with two disulfide bonds ($Cox17_{2S\text{-}S}$) and two reduced Cys residues, which bind one Cu(I) ion [$Cu_1(I)Cox17_{2S\text{-}S}$ hereafter]. In more reducing conditions, Cox17 exists in the fully reduced state, which binds cooperatively four Cu(I) ions forming a tetracopper-thiolate cluster [$Cu_4(I)Cox17$ hereafter] (23). In principle, both metallated forms of Cox17 could transfer metals to HSco1 protein.

To test which form of Cox17 can transfer Cu(I) to WT-HSco1, we have produced a mixture of $Cu_4(I)Cox17$ and $Cu_1(I)Cox17_{2S\text{-}S}$ forms and mixed it to reduced apoWT-HSco1. ESI-MS data of the Cox17 mixture showed metalation of apoWT-HSco1 with one Cu(I) ion and the concomitant decrease of the peak of $Cu_1(I)Cox17_{2S\text{-}S}$, whereas that of $Cu_4(I)Cox17$ remains unaltered (SI Fig. 11). This finding indicates that $Cu_1(I)Cox17_{2S\text{-}S}$ preferentially transfers Cu(I) to apoWT-HSco1. All of the subsequent NMR and ESI-MS experiments thus have been performed with the $Cu_1(I)Cox17_{2S\text{-}S}$ form.

Competition experiments for Cu(I) between the $Cox17_{2S\text{-}S}$ protein and the Cu(I) chelator DTT were carried out with ESI-MS technique as described in ref. 23. From these data, it results that $Cox17_{2S\text{-}S}$ bind one Cu(I) ion tightly with a $K_D$ value of $6.4 \pm 0.6 \times 10^{-15}$ M (SI Fig. 12).

When $^{15}$N-labeled apoWT-HSco1 is titrated with increasing amounts of unlabelled $Cu_1(I)Cox17_{2S\text{-}S}$ in the presence of 1 mM DTT, the intensity of some of its NH signals decreases in the $^1$H-$^{15}$N HSQC spectra, and, concomitantly, NH signals of the Cu(I)WT-HSco1 species appeared with increasing intensities along the titration (SI Fig. 13). No additional signals from a possible (transiently populated) intermediate could be detected at any point of the titration. ApoWT-HSco1 reaches 90% of its metalation upon addition of 1 eq of $Cu_1(I)Cox17_{2S\text{-}S}$, indicating a lower limit of the equilibrium constant of $10^2$. Considering the latter value and the $K_D$ value of $Cu_1(I)Cox17_{2S\text{-}S}$ ($K_D = 6.4 \pm 0.6 \times 10^{-15}$ M), $K_D$ of Cu(I)WT-HSco1 is estimated to be $\approx 10^{-17}$ or lower, thus WT protein displaying a higher affinity for Cu(I) compared with the mutant ($K_D = 3.2 \pm 0.6 \times 10^{-13}$ M). The rotational correlation time ($13.2 \pm 0.9$ ns) of WT-HSco1 in the 1:1 mixture with $Cu_1(I)Cox17_{2S\text{-}S}$ is not higher than that of isolated apo or Cu(I)WT-HSco1 ($13.8 \pm 1.6$ and $14.5 \pm 1.1$ ns, respectively), indicating that no complex is present at detectable concentrations. The copper(I) transfer process is slow on the chemical-shift time scale, setting a lower limit for the equilibration rate of $\approx 10^2\ s^{-1}$ [determined by the smallest chemical-shift difference between apoWT-HSco1 and Cu(I)WT-HSco1 that can be detected, i.e., $\approx$0.1 ppm at 800 MHz]. The comparison of the $^1$H-$^{15}$N HSQC spectra of the Cu(I)WT-HSco1 metalated via $Cu_1(I)Cox17_{2S\text{-}S}$ with that of Cu(I)WT-HSco1 metallated via Cu(I) acetonitrile complex (SI Fig. 14) shows that a few NH resonances (residues 164, 243, 245, 258, and 260–262) close to the metal-binding site are missing, broader, or having two conformational states in the former spectrum, indicating that Cox17 is transiently interacting with this region of WT-HSco1 producing conformational exchange processes of these NH resonances.

ESI-MS spectrometry confirms the NMR data, showing that, by adding an excess of $apoCox17_{2S\text{-}S}$, the apoWT-HSco1/Cu(I)WT-HSco1 ratio does not change (SI Fig. 15 *C* versus *B*), indicating that Cu(I) ion is bound to WT-HSco1 with higher affinity than to $Cu_1(I)Cox17_{2S\text{-}S}$. According to the different metal-binding affinities, from ESI-MS experiments, we also established that even 10 mM DTT cannot extract Cu(I) from Cu(I)WT-HSco1, whereas already 5 mM DTT extracts $\approx$40% of copper from $Cu_1(I)Cox17_{2S\text{-}S}$. Therefore, $Cox17_{2S\text{-}S}$ does not compete with WT-HSco1 for Cu(I) ions, but vice versa, it contributes to metalation of WT-HSco1 protein as it follows from the fact that $Cox17_{2S\text{-}S}$ shifts the metalation equilibrium of HSco1 toward the Cu(I)WT-HSco1 form more than the Cu(I)DTT complex does (SI Fig. 15 *A* and *B*). These data are in agreement with the copper content of human Sco1, determined from the cytoplasm of yeast cells overexpressing human Sco1 in the presence and absence of co-overexpression of human Cox17 (9).

ESI-MS spectra also indicate that, in the absence of metal ion, WT-HSco1 and Cox17 proteins do not form any complex. However, in the presence of 1 eq of Cu(I) there are two minor twin-peaks in the ESI-MS spectra (SI Fig. 15*D*) whose deconvolution yields molecular masses of 26,497 and 26,562 Da, which correspond to WT-HSco1/$Cu_1(I)$/$Cox17_{2S\text{-}S}$ and WT-HSco1/$Cu_2(I)$/$Cox17_{2S\text{-}S}$ complexes (theoretical $M_r$ 26,499.8 and 26,563.4 Da, respectively). These peaks have very low intensity, indicating that these complexes are transient and not highly populated states, in agreement with NMR results obtained at millimolar concentration. However, the relative intensity of these minor peaks increases at higher concentration of proteins, indicating that an equilibrium between free proteins and protein complexes is present. Moreover, at substoichiometric concentrations of Cu(I) ions, WT-HSco1/$Cu_1(I)$/$Cox17_{2S\text{-}S}$ is prevalent, whereas at higher Cu(I) concentrations, the WT-HSco1/$Cu_2(I)$/$Cox17_{2S\text{-}S}$ form prevails. This is another example of formation of a metal-mediated protein–protein complex, also observed in the case of other copper chaperones (24–26). As a whole, the ESI-MS results indicate that WT-HSco1/$Cu_1(I)$/$Cox17_{2S\text{-}S}$ is the transient intermediate involved in metal transfer from $Cu_1(I)Cox17_{2S\text{-}S}$ to WT-HSco1. At higher metal concentrations, WT-HSco1/$Cu_2(I)$/$Cox17_{2S\text{-}S}$ complex also exists, which suggests that the WT-HSco1/$Cox17_{2S\text{-}S}$ complex can accommodate two Cu(I) ions.

When $Cu_1(I)Cox17_{2S\text{-}S}$ is added to apoP174L-HSco1, differently from what happens for WT-HSco1, no copper transfer occurs at 1:1 $Cu_1(I)Cox17_{2S\text{-}S}$/P174L-HSco1 ratio, as judged by the $^1$H-$^{15}$N HSQC spectrum of the mixture. By increasing the $Cu_1(I)Cox17_{2S\text{-}S}$/P174L-HSco1 ratio up to 2:1, copper transfer occurs slowly on the chemical-shift time scale, similarly to the WT protein, but only $\approx$20% of P174L-HSco1 is metallated, accordingly to the higher affinity of $Cox17_{2S\text{-}S}$ for copper(I) [$K_D = 6.4 \pm 0.6 \times 10^{-15}$ M for $Cu_1(I)Cox17_{2S\text{-}S}$; $K_D = 3.2 \pm 0.6 \times 10^{-13}$ M for Cu(I)P174L-HSco1]. ESI-MS spectra also show that the addition of $Cox17_{2S\text{-}S}$ up to 3 eq does not improve the metalation of P174L-HSco1 (Fig. 1 *E* versus *D*), which is different from what occurs with the WT protein. Addition of $Cox17_{2S\text{-}S}$ also does not change the charge-state distribution of Cu(I)P174L-HSco1 (SI Fig. 16), which remains similar to that of apoP174L-HSco1 (Fig. 1*E*). Similarly to WT-HSco1, no protein–protein complexes are observed in ESI-MS spectra in the absence of metal, and a minor twin peak, corresponding to P174L-HSco1/$Cu_1(I)$/$Cox17_{2S\text{-}S}$ and P174L-HSco1/$Cu_2(I)$/$Cox17_{2S\text{-}S}$ complexes, is detected in ESI-MS spectrum in presence of Cu(I) ions (SI Fig. 16), which indicates that transient protein–protein complexes with 1 and 2 Cu(I) ions also do exist in case of the mutant protein. All of the data indicate that, even if Cox17 is still capable of interacting and exchanging copper(I) with the P174L-HSco1 mutant, the latter is not efficiently metallated into a compact copper(I) form, at variance with what occurs in WT protein.

## Discussion

Copper incorporation into CcO is biologically crucial; it is, however, an extremely complex process, which is tightly regulated and requires a large array of proteins, each of them with

a specific, in most of the cases, nonreplaceable role. The comprehension and description of these processes are still in their infancy, and only now knowledge about the structure and functional role of the assisting proteins has begun to become available. Many lines of evidence show that copper insertion into $Cu_A$ site of COXII subunit is not a simple, passive copper transfer from Cox17 to Sco1/2 proteins and finally to COXII, but redox reactions are interlinked with the process of copper transfer (12, 15, 16, 27).

In this work, we have shown that the P174L mutation in HSco1 significantly affects the redox and metal-binding properties of this protein. Structurally, the mutation produces the lack of well organized hydrophobic contacts and a structural heterogeneity in the vicinity of the metal-binding region. The local structural changes induced by the point mutation decrease the copper(I) affinity of the mutant, thus negatively affecting the cometallochaperone function of HSco1 in the $Cu_A$ assembly. The mutation also determines that the oxidation and reduction rates of the disulphide bond of the mutant are much slower than those of the WT protein. It is likely that introduction of the bulky Leu-174 disturbs the mutual orientation of cysteines and slows down the local conformational changes necessary for disulfide bond formation and disruption. The thioredoxin role of HSco1, proposed for maintaining the receiving $Cu_A$ site in the suitable reduced state (15, 16), therefore is significantly perturbed because the mutation could slow down the reduction of the copper-binding cysteines in $Cu_A$ site of CcO. Overall, these alterations induced by the mutation on copper-binding and redox properties of HSco1 can sizably decrease the efficiency of the copper transfer from Cu(I)HSco1 to the $Cu_A$ site of CcO.

Our results also provide a detailed understanding of the metalation process of HSco1 by Cox17 and show how the mutation at position 174 of HSco1 affects this process. ESI-MS data demonstrate that $Cu_1(I)Cox17_{2S\text{-}S}$, but not $Cu_4(I)Cox17$, is capable of transferring Cu(I) to apoWT-HSco1 and that minor amounts of the metal-bridged species, WT-HSco1/$Cu_1(I)$/$Cox17_{2S\text{-}S}$ and WT-HSco1/$Cu_2(I)$/$Cox17_{2S\text{-}S}$, do occur, which are probably the transient intermediates involved in the metal transfer from $Cu_1(I)Cox17_{2S\text{-}S}$ to apoWT-HSco1. Such transient interaction with $Cox17_{2S\text{-}S}$ assists WT-HSco1 to pass from the open to the closed state, which binds Cu(I) ions extremely strongly (Fig. 4). The mutant P174L-HSco1 behaves differently: the conformational disorder experienced by Cu(I)P174L-HSco1 indeed is associated with a weakly bound metal (Fig. 4), and $Cox17_{2S\text{-}S}$ is not able to assist the mutant P174L-HSco1 to form the more compact state as it happens with WT-HSco1.

In conclusion, the P174L mutation in HSco1 decreases the efficiency of both metal-binding and redox properties of HSco1, which both are potentially involved in HSco1-mediated transfer of the copper and electrons from Cox17 to the $Cu_A$ site of COXII (16).

## Methods

**Protein Expression and Characterization.** The pathogenic mutation at the gene position C520T, corresponding to P174L amino acid change, was made by using QuikChange mutagenesis kit (Stratagene, La Jolla, CA). WT-HSco1 protein and P174L-HSco1 pathogenic mutant were produced in *E. coli* BL21-Gold(DE3) (Stratagene) following an already reported protocol (16). Porcine Cox17 was isolated from porcine intestine as fully oxidized apo protein ($Cox17_{3S\text{-}S}$) and lyophilized (23).

The oxidation state of the cysteines of the WT- and P174L-HSco1 proteins was evaluated through the selective reaction of the free thiol groups with 4-acetamido-4-maleimidylstilbene-2,2-disulfonic acid, which adds ≈500 Da per reactive thiol to the total mass, thus shifting the mobility of the protein on a SDS/PAGE denaturing gel. The metal content was determined by inductively coupled plasma mass spectrometry. Far-UV CD spectra (185–260 nm) were recorded on a Jasco J-810 spectropolarimeter on 10 $\mu$M protein solutions in 20 mM phosphate buffer, pH 7.2, at 298 K.

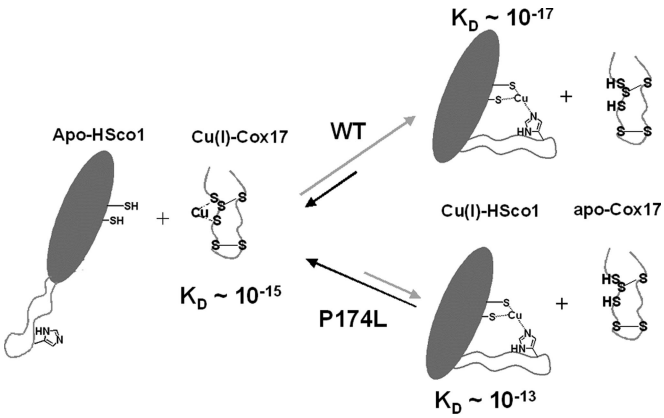


**Fig. 4.** The effect of the P174L-Sco1 mutation in the copper transfer with Cox17. The pathogenic human Sco1 mutation P174L, next to the copper-binding motif, determines a reduction of the efficiency of the copper transfer from the mitochondrial metallochaperone Cox17 to Sco1.

The melting temperatures of WT- and P174L-HSco1 proteins in the apo state were determined through the fluorescence-based thermal-shift assay (28). Fluorescence intensity was measured at different temperatures with excitation/emission wavelengths of 490 and 575 nm, respectively.

Redox equilibration between WT- or P174L-HSco1 and glutathione was followed through the change of fluorescence monitored on 5 $\mu$M concentrations of protein samples previously incubated for at least 6 h under an $N_2$ atmosphere, with different reduced/oxidized glutathione (GSH/GSSG) ratios (0.01 mM GSSG and varying concentrations of GSH, 0.1–200 mM) in 50 mM phosphate buffer, pH 7.2. The collection and data analysis was performed by following a protocol previously described for thioredoxins (29).

**Preparation of Cox17, HSco1, and P174L-HSco1 Samples for MS Measurements.** For MS experiments, purified WT- and P174L-HSco1 proteins containing one disulfide bond were brought into 50 mM ammonium acetate, pH 7.5, by using HiPrep26/10 desalting column (Amersham Biosciences, Uppsala, Sweden). Lyophilized $Cox17_{3S\text{-}S}$ was dissolved in argon-saturated 50 mM ammonium acetate, pH 7.5, at 75 $\mu$M concentration, and this stock solution was used for further experiments. $Cox17_{2S\text{-}S}$ was produced by reduction of $Cox17_{3S\text{-}S}$ with 1 mM DTT at 298 K (incubation time 2 min), which leads to reduction of one most labile disulfide bond in $Cox17_{3S\text{-}S}$. Fully reduced Cox17 was prepared by incubation of $Cox17_{3S\text{-}S}$ with 1 mM DTT at 45°C for 100 min.

**MALDI-TOF and ESI-MS Protein Characterization.** In MALDI-TOF experiments, reduction of oxidized apoWT-HSco1 and apoP174L-HSco1 (2 $\mu$M protein concentration) by 1 mM DTT was followed in 50 mM ammonium acetate buffer, pH 7.5, by stopping the reduction with 5 mM iodoacetamide. Protein adducts were identified by MALDI-TOF MS on a Voyager STR instrument (Applied Biosystems, Foster City, CA).

In ESI-MS experiments, 0.8–4.8 $\mu$M concentrations of protein samples or mixtures were infused by a syringe pump at 15 $\mu$l/min into an Ettan API ESI-TOF mass spectrometer (Amersham Biosciences). Mass spectra were recorded during 2 to 3 min at a capillary exit voltage of 150 V. HSco1 and P174L-HSco1 were reduced with 1.0 mM DTT at 298 K. ESI-MS spectrum of P174L-HSco1 also exposed two minor peaks corresponding to incorrectly cleaved protein forms, which did not disturb measurements. Reconstitution of HSco1 and Cox17 forms with

copper was conducted as follows. First, Cu(II) acetate was dissolved at 150 $\mu$M concentration in argon-saturated 50 mM ammonium acetate, pH 7.5, and Cu(II) was reduced to Cu(I) by addition of 1.0 mM DTT. Different equivalents of freshly prepared Cu(I)DTT complex were added to HSco1 or Cox17 and incubated in buffer with 1.0 mM DTT, and the mixture was incubated for additional 1 min at 25°C, and ESI-MS spectra were recorded as described above. In Cox17/HSco1 titration experiments, $Cu_1(I)Cox17_{2S\text{-}S}$ was prepared by addition of Cu(I) to $Cox17_{2S\text{-}S}$, which subsequently was mixed with a sample of HSco1 protein. All buffers contained 1 mM DTT. The dissociation constant of $Cu_1(I)Cox17_{2S\text{-}S}$ complex has been calculated as previously reported (23).

**NMR Protein Characterization.** The fully copper-loaded state of the $Cu_1(I)$P174L-HSco1 NMR sample used for structure determination has been produced by adding 1.5 eq of $[Cu(I)(CH_3CN)_4]PF_6$ complex to reduced apo protein in 50 mM phosphate buffer at pH 7.2 and in the absence of DTT. NMR spectral assignment and structure determination of $Cu_1(I)$P174L-HSco1 were obtained through the experiments listed in SI Table 1. The $^1H$, $^{13}C$, and $^{15}N$ resonance assignments of the $Cu_1(I)$P174L-HSco1 are reported in SI Table 2. After conversion of the NMR data in structural restraints, the structure was calculated by using the program DYANA. The relative intensity of the split resonances was taken into account when converting NOE volumes into distances. The best 30 conformers of the DYANA family were subjected to restrained energy minimization (REM) with AMBER 8.0, by using the metal force field already applied for WT-HSco1 (16). The statistical analysis of the REM family of $Cu_1(I)$P174L-HSco1 structures is reported in SI Table 3. The programs PROCHECK, PROCHECK-NMR (30, 31), and WHATIF (32) were used in the evaluation of the quality of the structures. More than 90% of residues were located in the allowed regions of the Ramachandran plot.

Titrations of $^{15}N$-labeled apoHSco1 (0.1 mM) and apoP174L-HSco1 (0.1 mM) with unlabelled $Cu_1(I)Cox17_{2S\text{-}S}$ or $[Cu(I)(CH_3CN)_4]PF_6$ were performed with NMR spectroscopy following the $^1H$-$^{15}N$ spectral changes in HSQC spectra upon addition of increasing amounts of the unlabelled protein partner or copper(I) complex in the presence of 1 mM DTT. Aliquots were added in a Coy chamber under nitrogen atmosphere at 298 K. The metalation state of WT-HSco1 and P174L-HSco1 proteins was monitored along the NMR titration through a few residues that are next to the copper(I) binding motif CXXXC and therefore are experiencing chemical shifts sensitive to the metalation state. In addition, their NHs are not overlapped in the $^1H$-$^{15}N$ HSQC maps, thus they are easily integrated during the titration steps to estimate the relative population of apo and copper(I) loaded forms, which allows the estimation of the metal affinity. The dissociation constant $K_D$ of Cu(I)P174L-HSco1 is obtained according to the following scheme:

$$\text{Cu(I)P174L-HScol} + \text{DTT} \Leftrightarrow \text{apoP174L-HScol} + \text{Cu(I)DTT}. \quad [1]$$

The conditional dissociation constant for the Cu(I)DTT complex, necessary for the above $K_D$ estimation, is $6.31 \times 10^{-12}$ M at pH = 7.4 and $T$ = 298 K (33).

$R_1$ and $R_2$ $^{15}N$ relaxation rates on 1:1 $Cu_1(I)Cox17$/WT-HSco1 mixture were measured at 298 K on a Bruker (Billerica, MA) Avance 500 spectrometer and then analyzed by using a standard procedure (34). An estimate of the overall rotational correlation time was derived from the measured $R_2/R_1$ ratio.

This work was supported by Marie Curie Host fellowships for early stage research training ("NMR in Inorganic Structural Biology" Fellowship MEST-CT-2004-504391), the European Community (EU-NMR Contract 026145), Estonian Science Foundation Grant 5635, and a grant from Ente Cassa di Risparmio di Firenze (to FiorGen Foundation).

1. Carr HS, Winge DR (2003) *Acc Chem Res* 36:309–316.
2. Nobrega MP, Bandeira SCB, Beers J, Tzagoloff A (2002) *J Biol Chem* 277:40206–40211.
3. Barros MH, Johnson A, Tzagoloff A (2004) *J Biol Chem* 279:31943–31947.
4. Glerum DM, Shtanko A, Tzagoloff A (1996) *J Biol Chem* 271:20531–20535.
5. Beers J, Glerum DM, Tzagoloff A (2002) *J Biol Chem* 277:22185–22190.
6. Lode A, Kuschel M, Paret C, Rodel G (2000) *FEBS Lett* 485:19–24.
7. Mattatall NR, Jazairi J, Hill BC (2000) *J Biol Chem* 275:28802–28809.
8. Andruzzi L, Nakano M, Nilges MJ, Blackburn NJ (2005) *J Am Chem Soc* 127:16548–16558.
9. Horng YC, Leary SC, Cobine PA, Young FB, George GN, Shoubridge EA, Winge DR (2005) *J Biol Chem* 280:34113–34122.
10. Nittis T, George GN, Winge DR (2001) *J Biol Chem* 276:42520–42526.
11. Horng YC, Cobine PA, Maxfield AB, Carr HS, Winge DR (2004) *J Biol Chem* 279:35334–35340.
12. Arnesano F, Banci L, Bertini I, Martinelli M (2005) *J Proteome Res* 4:63–70.
13. Balatri E, Banci L, Bertini I, Cantini F, Ciofi-Baffoni S (2003) *Structure (London)* 11:1431–1443.
14. Williams JC, Sue C, Banting GS, Yang H, Glerum DM, Hendrickson WA, Schon EA (2005) *J Biol Chem* 280:15202–15211.
15. Ye Q, Imriskova-Sosova I, Hill BC, Jia Z (2005) *Biochemistry* 44:2934–2942.
16. Banci L, Bertini I, Calderone V, Ciofi-Baffoni S, Mangani S, Martinelli M, Palumaa P, Wang S (2006) *Proc Natl Acad Sci USA* 103:8595–8600.
17. Shoubridge EA (2001) *Am J Med Genet* 106:46–52.
18. Valnot I, Osmond S, Gigarel N, Mehaye B, Amiel J, Cormier-Daire V, Munnich A, Bonnefont JP, Rustin P, Rotig A (2000) *Am J Hum Genet* 67:1104–1109.
19. Paret C, Lode A, Krause-Buchholz U, Rodel G (2000) *Biochem Biophys Res Commun* 279:341–347.
20. Cobine PA, Pierrel F, Leary SC, Sasarman F, Horng YC, Shoubridge EA, Winge DR (2006) *J Biol Chem* 281:12270–12276.
21. Eyles SJ, Kalatshov IA (2004) *Methods* 34:88–99.
22. Aslund F, Berndt KD, Holmgren A (1997) *J Biol Chem* 272:30780–30786.
23. Palumaa P, Kangur L, Voronova A, Sillard R (2004) *Biochem J* 382:307–314.
24. van Dongen EM, Klomp LW, Merkx M (2004) *Biochem Biophys Res Commun* 323:789–795.
25. Banci L, Bertini I, Cantini F, Felli IC, Gonnelli L, Hadjiliadis N, Pierattelli R, Rosato A, Voulgaris P (2006) *Nat Chem Biol* 2:367–368.
26. Strausak D, Howie MK, Firth SD, Schlicksupp A, Pipkorn R, Multhaup G, Mercer JF (2003) *J Biol Chem* 278:20821–20827.
27. Imriskova-Sosova I, Andrews D, Yam K, Davidson D, Yachnin Y, Hill BC (2006) *Biochemistry* 44:16949–16956.
28. Lo MC, Aulabaugh A, Jin G, Cowling, R, Bard J, Malamas M, Ellestad G (2004) *Anal Biochem* 332:153–159.
29. Haugstetter J, Blicher T, Ellgaar L (2005) *J Biol Chem* 280:8371–8380.
30. Laskowski RA, Rullmann JAC, MacArthur MW, Kaptein R, Thornton JM (1996) *J Biomol NMR* 8:477–486.
31. Laskowski RA, MacArthur MW, Moss DS, Thornton JM (1993) *J Appl Crystallogr* 26:283–291.
32. Vriend G (1990) *J Mol Graphics* 8:52–56.
33. Krezel A, Lesniak W, Jezowska-Bojczuc M, Mlynarz P, Brasun J, Kozlowski H, Bal W (2001) *J Inorg Biochem* 84:77–88.
34. Peng JW, Wagner G (1992) *J Magn Reson* 98:308–332.